

## Detection and quantification of broadleaf weeds in turfgrass using close-range multispectral imagery with pixel- and object-based classification

Daniel S. Hahn, Peter Roosjen, Alejandro Morales, Jelmer Nijp, Leslie Beck, Ciro Velasco Cruz & Bernd Leinauer

To cite this article: Daniel S. Hahn, Peter Roosjen, Alejandro Morales, Jelmer Nijp, Leslie Beck, Ciro Velasco Cruz & Bernd Leinauer (2021) Detection and quantification of broadleaf weeds in turfgrass using close-range multispectral imagery with pixel- and object-based classification, International Journal of Remote Sensing, 42:21, 8035-8055, DOI: [10.1080/01431161.2021.1969058](https://doi.org/10.1080/01431161.2021.1969058)

To link to this article: <https://doi.org/10.1080/01431161.2021.1969058>



© 2021 The Author(s). Published by Informa UK Limited, trading as Taylor & Francis Group.



Published online: 02 Oct 2021.



[Submit your article to this journal](#)



Article views: 405



[View related articles](#)



[View Crossmark data](#)

# Detection and quantification of broadleaf weeds in turfgrass using close-range multispectral imagery with pixel- and object-based classification

Daniel S. Hahn<sup>a</sup>, Peter Roosjen<sup>b</sup>, Alejandro Morales<sup>a,c</sup>, Jelmer Nijp<sup>d</sup>, Leslie Beck<sup>e</sup>,  
Ciro Velasco Cruz<sup>e</sup> and Bernd Leinauer <sup>a,e</sup>

<sup>a</sup>Centre for Crop Systems Analysis, Wageningen University & Research, Wageningen, The Netherlands; <sup>b</sup>Laboratory of Geo-Information Science and Remote Sensing, Wageningen University & Research, Wageningen, The Netherlands; <sup>c</sup>Plant Ecophysiology and Molecular Plant Physiology, Utrecht University, Utrecht, The Netherlands; <sup>d</sup>Ecohydrology Department, KWR Water Research Institute, Nieuwegein, The Netherlands; <sup>e</sup>Department of Extension Plant Sciences, New Mexico State University, Las Cruces, USA

## ABSTRACT

The current practice used to evaluate broadleaf weed cover in turfgrass is visual assessment, which is time consuming and often leads to inconsistencies among evaluators. In this study, we investigated the effectiveness of constructing Random Forest models (RF), either pixel-, object-based (OBIA) or a combination of both to detect and quantify broadleaf weed cover. High resolution multispectral images were captured of 136 turfgrass plots, seeded with five species of *Festuca* L. and overseeded with either clover (*Trifolium repens* L.), daisy (*Bellis perennis* L.), yarrow (*Achillea millefolium* L.), or a mixture of all three weeds. Ground measurements of vegetation cover and bare soil were taken with a point quadrat and digital image analysis. Weeds were detected with 99% accuracy by OBIA, followed by the combined approach (98%) and Pixel-based approach (93%). Accuracy at distinguishing among weed species was somewhat lower (89%, 81% and 90%, respectively), with yarrow contributing most to the decrease in accuracy. The predictions based on ground measurements were further compared to field measurements. For both soil and weed classification, models that used shape features (OBIA and combined) resulted in better agreement with field measurements compared to Pixel-based classifications. Our study suggests that broadleaf weed cover comprised of species such as clover and daisy can be accurately quantified with high resolution multispectral images; however, quantifying yarrow cover remains challenging.

## ARTICLE HISTORY

Received 5 May 2021  
Accepted 11 August 2021

## 1. Introduction

The presence of weeds disrupts the playing quality and aesthetic appearance of turfgrass areas (Larsen, Kristoffersen, and Fischer 2004; McCarthy and Murphy 1994; McElroy and Martins 2013). Since the development of selective herbicides such as 2,4-D (2,4-dichlorophenoxyacetic

**CONTACT** Bernd Leinauer  [leinauer@nmsu.edu](mailto:leinauer@nmsu.edu)  Centre for Crop System Analysis, Wageningen University & Research, Droevendaalsesteeg 1, Wageningen 6708 PB, The Netherlands

© 2021 The Author(s). Published by Informa UK Limited, trading as Taylor & Francis Group.  
This is an Open Access article distributed under the terms of the Creative Commons Attribution-NonCommercial-NoDerivatives License (<http://creativecommons.org/licenses/by-nc-nd/4.0/>), which permits non-commercial re-use, distribution, and reproduction in any medium, provided the original work is properly cited, and is not altered, transformed, or built upon in any way.

acid) (Marth and Mitchell 1944), herbicides have become the main tool used by managers to control weeds in turfgrass (Dahl Jensen et al. 2017; Hatcher and Froud-Williams ; Heap 2014; McElroy and Martins 2013).

The European Union actively promotes the use of alternative non-chemical products or techniques to control weeds (European Parliament 2009) because of potential health risks associated with exposure to herbicides (Kim, Kabir, and Jahan 2017), environmental concerns (Aktar, Sengupta, and Chowdhury 2009) and the increasing risk of herbicide resistance due to overuse (De Prado and Franco 2004). Turfgrass managers are encouraged to adopt integrated pest management (IPM) approaches to reduce the input of herbicides (Busey 2003). However, a lack of established weed treatment thresholds, and the absence of time efficient, low-cost alternative control methods limit the ability of turfgrass managers to follow clear IPM protocols (Latimer et al. 1996). Management practices such as increasing mowing heights and nitrogen fertilization enhance the competitiveness of turfgrass against weeds (Voight, Fermanian, and Haley 2001), but full weed suppression generally requires the use of herbicides (Busey 2003).

Remote sensing tools used in precision agriculture could be designed to detect and treat localized high weed densities in turfgrass, thereby reducing the overall herbicide loads required to control weeds (Zhang and Kovacs 2012). In addition to reducing herbicide use on turfgrass areas, automated weed detection systems could also help turfgrass breeders accurately assess the competitiveness of grasses against weeds. Currently, turfgrass breeders typically use visual scores to assess turfgrass quality or weed cover (Bunderson et al. 2009; Kaur et al. 2016; National Turfgrass Evaluation Program 2020). However, visual scoring is subjective, time consuming, and can be inconsistent over time and amongst evaluators. As a result, the reproducibility of such data has been questioned (Horst, Engelke, and Meyers 1984; Leinauer et al. 2014; Trenholm, Carrow, and Duncan 1999). Regardless, in the absence of high throughput alternatives, breeders and turfgrass scientists still rely on visual assessments to quantify weed cover and turfgrass quality.

Digital image analysis has been adopted by some turfgrass scientists to quantify vegetation cover and turfgrass quality. High values obtained from dark green colour index (DGCI) analysis correlate strongly to high chlorophyll content and genetically desirable dark green colour of cultivars (Karcher and Richardson 2013). This technology can readily distinguish vegetation from soil but cannot discriminate between desirable plants and weeds.

In situ strategies to objectively separate vegetation cover includes the use of point-based reflectance data collected by hand-held spectroradiometers. This method has been successfully used to distinguish two grassy weed species, dallisgrass (*Paspalum dilatatum* Poir.) and southern crabgrass (*Digitaria ciliaris* (Retz.) Koeler), and two broadleaf weed species, namely virginia buttonweed (*Diodia virginiana* L.) and eclipta (*Eclipta prostrata* (L.) L.), from a variety of warm and cool season turfgrasses (Hutto et al. 2006). However, this procedure is labour intensive and requires expensive equipment to collect the hyper-spectral data. An additional disadvantage is that spectroradiometry measurements are point observations, which cannot be used to map spatial distribution of weeds. Remotely sensed data may offer a solution to these limitations by providing an empirical, cost-effective and reliable source of data that could detect and distinguish weeds from turfgrass, and map their spatial distribution. In recent years, the development and

application of novel algorithms to analyse remotely sensed imagery in combination with increased computational power and ease of data acquisition via unmanned aerial vehicles, has led to considerable advances in the use of remote sensing techniques (Ma et al. 2015; Gómez, White, and Wulder 2016; Mulla 2013). Remote sensing is used in a large variety of applications at spatial scales ranging from individual plants to fields. Examples include the estimation of plant-specific parameters such as leaf area index, chlorophyll content, and canopy cover (Roosjen et al. 2018; Yang et al. 2017), and the assessment of characteristics such as ground cover, vegetation type, and drought stress, to name a few (Gómez, White, and Wulder 2016; Nijp et al. 2019; Olmstead et al. 2004).

Using remotely sensed imagery followed by colour modelling, Tang et al. (2016) were able to identify weed-covered areas in crop rows of agricultural fields with 92% overall accuracy (OA). While we acknowledge that OA provides a limited perspective on classification accuracy, it can be used for approximate comparisons (Alberg et al. 2004). Huang et al. (2018) demonstrated how remote sensing tools could provide a time and labour-saving alternative to ground collected spectral reflectance data or digital image analysis for the assessment of weed density in agricultural settings. In agricultural studies, hyperspectral radiometry and multispectral aerial imagery have been successfully used to quantify johnsongrass (*Sorghum halepense* (L.) Pers.), which is also a problematic turfgrass weed (Thorpe and Tian 2004). Yu et al. (2020) tested the performance of deep convolutional neural networks to detect a variety of grassy weeds, including crabgrass (*Digitaria* spp.), in a bermudagrass sward, yielding high overall precision (>93% of grassy weed species). However, detection performance was dependent on the algorithm used and decreased considerably with reduced abundances of weeds likely caused by pixel mixing resulting in classification error (Yu et al. 2020; Hsieh, Lee, and Chen 2001).

Other approaches used to separate and map different types of vegetation include utilizing contextual information derived from object-based image analysis (OBIA), which may improve the accuracy of discerning among vegetation classes of interest beyond pixel-based reflectance patterns (Blaschke et al. 2014). One example was the detection of bermudagrass (*Cynodon dactylon* (L.) Pers.) in vineyards using multispectral aerial images and OBIA (Jiménez-Brenes et al. 2019). Given that spectral characteristics of weeds and grasses differ very little whereas their shapes and texture can vary greatly (Weis et al. 2009), OBIA shows potential for accurate detection of broadleaf weeds in turfgrass. One challenge of detecting broadleaf weeds in turfgrass is the small size of some species, depending on their growth stage.

Currently, no reliable, affordable methods based on digital imagery exist to detect, quantify and map broadleaf weed cover in turfgrass areas with a high degree of spatial resolution. Research is needed to assess the usefulness of OBIA or pixel-based classification in detecting and quantifying broadleaf weeds in closely mowed turfgrass settings wherein differences in shape and spectral characteristics among species are minute. The objective of our study was to investigate the effectiveness of OBIA- and pixel-based classification derived from multispectral imagery at distinguishing among broadleaf weeds, grasses and soil. To that end, we compared the performance of OBIA and pixel-based classification methods using high-resolution imagery collected in a controlled field experiment that included five species of *Festuca* and three common European broadleaf weed species.

## 2. Materials and methods

### 2.1. Field trial

To explore the potential of using remote sensing techniques to distinguish and map percentage cover of weeds, grass and soil, we collected remotely sensed imagery data from a field experiment conducted at the Barenbrug Turfgrass Research Station in Wolfheze, The Netherlands (52°00'N, 5°47'E). The soil consisted of 79% sand, 12% silt and 3% clay, 6.4% organic matter and had a pH of 5 in the upper 15 cm of the soil profile. The study area was located within the controlled traffic region (CTR) of Deelen Airport in Arnhem, The Netherlands (52°03'N, 5°52'E). The experiment was initiated to investigate the competitiveness of fescue cultivars (sown on 13 July 2018), against three common turf weeds that were sown on 27 July 2018.

Treatments included six *Festuca* cultivars, namely Chewings fescue [*Festuca rubra* L. ssp. *fallax* (Thuill.) Nyman 'Musica'], hard fescue (*Festuca brevipila* Tracey 'Mentor'), slender creeping red fescue [*Festuca rubra* L. ssp. *littoralis* (G. Mey.) Auquier 'Samanta'], strong creeping red fescue (*Festuca rubra* L. *rubra* 'Barpearl' and 'Barisse'), and tall fescue [*Schedonorus arundinaceus* (Schreb.) Dumort., nom. cons. 'Melyane']. With the exception of grass controls, all plots sown with grass were oversown with weed treatments including either clover, daisy, yarrow or a mixture of all three weed species. The experiment included six cultivars oversown with weed seeds, six grass controls (grass cultivars only) and four weed controls (weed seeds only) All treatments were replicated four times. The individual plots measured 1.5 × 1.5 m and were arranged in a randomized complete block design.

Fescue cultivars were sown at a density of 20,150 seeds per m<sup>2</sup>, following guidelines by Beard (1973) and weeds were sown at a density of 6,200 seeds per m<sup>2</sup>. Granular fertilizer (NPK 12–10–18, Arm, Eurosolids, Westmaas, The Netherlands) was applied to the plots 28, 42, 56 and 72 days after sowing (DAS) the grass seeds at a rate of 200 kg ha<sup>-1</sup>. The field was rolled 21 DAS and mowed for the first time at 20 mm. From 28 DAS onwards, the field was mowed twice per week with a Jacobson TR3 reel mower (TR3, Jacobson, Racine, United States) at a cutting height of 15 mm, with clippings returned. We achieved uniform establishment of grasses and weeds 82 DAS. Before data collection dew and clippings were removed with a hand blower.

### 2.2. Data collection

Percent weed and vegetation cover of 136 experimental plots was measured 84 DAS. To determine the percentage of each plot covered by weeds (i.e. weed cover), a point quadrat frame was constructed with wires spaced 10 cm apart creating a mesh with 100 intersections (Laycock 1980). The frame was placed in the middle of each plot and presence or absence of weeds underneath each intersection was recorded on 3 October 2018. Similar methods were used by Gaussoin and Branham (1989) and Proctor, Weisenberger, and Reicher (2015). On the same day, total vegetation cover (i.e. weeds and grasses) of each plot was determined by photographing them using a lightbox. The custom-made lightbox was a 60 × 50 × 50 cm metal box with a hole

on the top large enough to insert a digital camera. Four lamps (5000 k colour and 450 lumen) were arranged inside the lightbox to produce consistent lighting conditions during image capturing, similar to methods used by (Karcher and Richardson 2013).

Images were taken with the digital camera (Canon Power shot SX 200 IS, Canon, Tokyo, Japan). Manual settings used were ISO 200, Aperture 2.6 and shutter speed 1/60 s, which provided the highest image quality in combination with the lightbox. The images were processed using the software Turf Analyser (Turf Analyser 2018), which applies a green pixel recognition algorithm to calculate the percentage of green vegetation in images. To determine non-vegetation cover (i.e. *bare soil*) for each plot, we subtracted the green pixels computed by Turf Analyser from the total pixels.

Weed cover measurements obtained with the point quadrat method and bare soil measurements obtained from the lightbox images and the Turf Analyser methods are referred to as 'observed data.' The observed data can be considered the quantitative industry standard, which are recorded on the ground. The following sections describe a new proposed methodology, which will be referred to as 'predicted data' using an airborne camera system to capture multispectral images and analysis by random forest models (RF classification) to determine weed cover and percentage bare soil.

Multispectral images of the field experiment were collected with a Parrot Sequoia+ camera (Parrot Sequoia+, Parrot, Paris, France). The camera collected images of 1280 × 960 pixels at four spectral bands: green (550 nm), red (660 nm), red edge (735 nm), and near infrared (NIR, 790 nm). In the field, prior to the image collection, calibration images were taken of a grey reference panel (Parrot Sequoia Calibration Target, Parrot, Paris, France) with known reflectance values (green: 18.4%, red: 19.7%, red edge: 22.7%, NIR: 27.6%) at the same spectral bands as the camera. To accurately geo-reference the images, 30 ground control points (GCPs) were placed in the field and their GPS coordinates measured with a Real Time Kinematic unit (HiPerV, Topcon, Tokyo, Japan), which has a horizontal and vertical accuracy of 5 mm + 0.5 ppm and 10 mm + 0.8 ppm, respectively.

The sequoia camera is designed to be used with an unmanned aerial vehicle (UAV). Because our study site was located in CTR of Deelen Airport, permission to fly a UAV was not obtained at the time of image acquisition. Therefore, the camera was dismantled from a set-up with a UAV and attached to a three-metre pole with the downwelling light sensor pointing upward to the sky and the camera towards the ground. Both sensor and camera were undisturbed by shade and were positioned parallel to the ground simulating the original UAV set-up. The pole itself was attached to a platform four-wheeled vehicle which was manually pushed across the research area to take images from 2.5 m above ground level (AGL), resulting in a ground sample distance (GSD) of 2.8 mm/pixel. Images were collected every two seconds with a forward and sideward overlap of approximately 95% and 80%, respectively, resulting in a uniform coverage of the study area. The images were taken under partially clouded conditions on 3 October, at 10 am (CEST). A total of 807 images were collected from the experimental area. The internal GPS of the camera stored the coordinates from which each image was taken. After data collection, we began image processing following the workflow outlined in [Figure 1](#), which will be explained in more detail in the following sections.

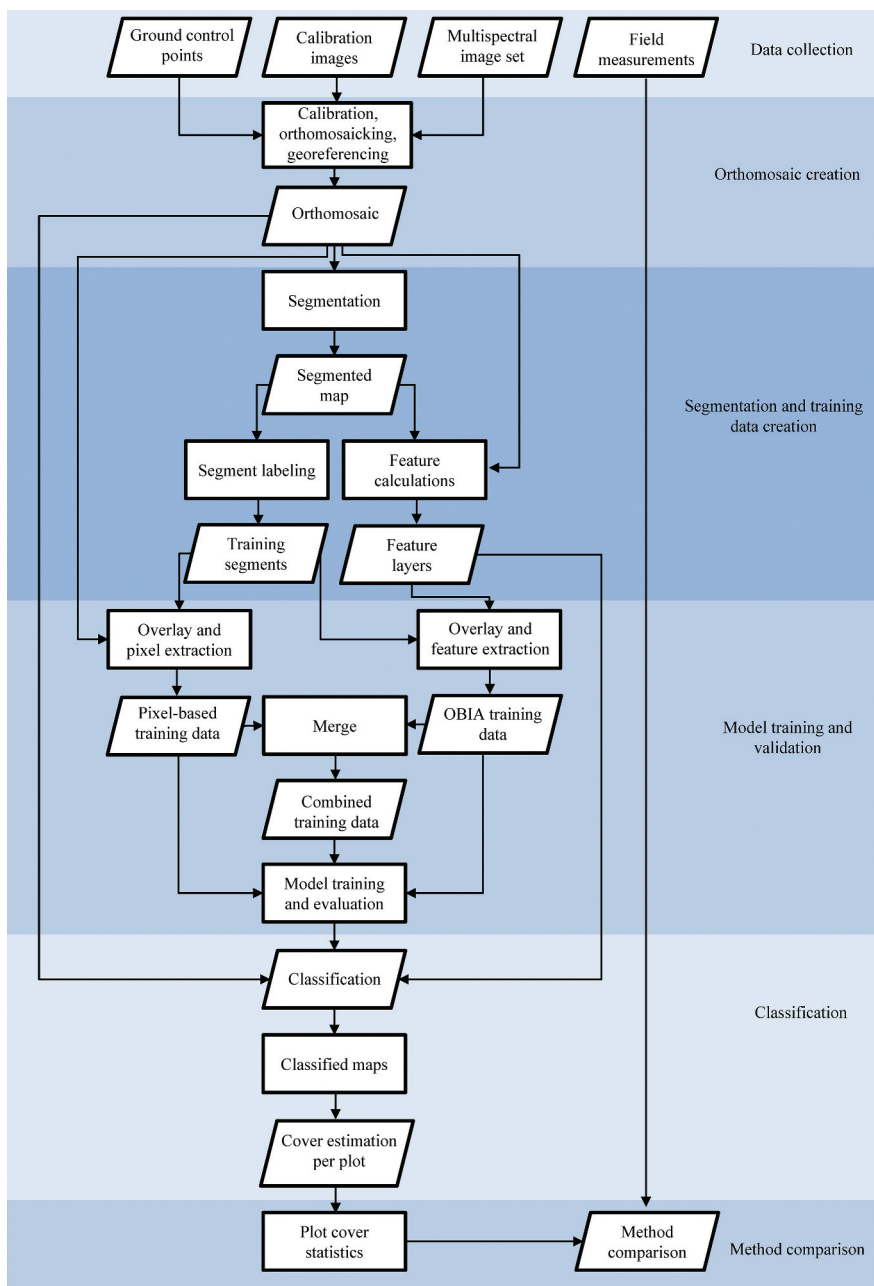


**Figure 1.** Project workflow from constructing object-based image analysis (OBIA), pixel based and combined models to classify vegetation cover. Rectangles indicate processes and parallelograms show products. The figure lists all steps from data collection (field measurements and multispectral image collection) to construction of the models and final comparisons between model data and ground measurements.

### 2.3. Orthomosaic creation

The multispectral images obtained were used to create an orthomosaic, using AgiSoft Metashape version 1.5.2 (AgiSoft LLC, St. Petersburg, Russia). An orthomosaic is a large image that is created by combining many georeferenced small images (Brown 1992; Laganieri 2000). First, pixel values of all four bands were calibrated using the measurement of the grey reference panel. The images were subsequently aligned at the *highest* accuracy setting using GPS data of the images and the GCPs. A dense point cloud was built at *medium* quality-setting without depth filtering. From this, an orthomosaic containing the four spectral bands was constructed with a ground pixel size of 3 mm.

### 2.4. Orthomosaic segmentation

The orthomosaic image was segmented in GRASS GIS 7.4.4 (GRASS Development Team 2017). Image segmentation groups adjacent pixels that are similar into segments, which are referred to as objects. The segmentation algorithm was driven by two parameters: 1) the minimal segment size, which is the minimum number of pixels that each segment can comprise and 2) a similarity parameter, which describes how similar pixels should be before they are assigned to a segment. For the segmentation process of the orthomosaic, we used a minimum segment size of 10 pixels and a similarity threshold of 0.025, respectively. After testing several combinations of these parameters, these values gave the best segmentation results. After segmentation of the orthomosaic, 1022 segments were manually labelled as grass (referred to as '*grass*'), no vegetation cover (referred to as '*soil*') or weed species (referred to as either '*clover*,' or '*daisy*,' or '*yarrow*') (Table 1).

### 2.5. Random forest models to classify vegetation

For our study we used RF classifications to sort vegetation, which are frequently used to categorize remotely sensed imagery, and other than the traditional Maximum Likelihood classification, do not rely on data distribution assumptions (Brodley and Friedl 1997; Nitze, Schulthess, and Asche 2012). Random forest models tend to classify weeds better than alternatives and have been used to successfully detect weeds, such as Camomile (*Chamaemelum nobile* L.) and Thistle (*Cirsium arvense* L.), in aerial images of agricultural fields sown with oats (Gašparović et al. 2020). For RF classification, training data are

**Table 1.** Number of annotated segments and pixels within each segment, separated by vegetation class. Segments were selected from an orthoimage of a field trial. Data from annotated segments were extracted to create the training data for vegetation classification models.

Class	Segments	Pixels
Clover	295	6964
Daisy	196	4968
Grass	167	502572
Soil	227	39746
Yarrow	137	3975

randomly selected, followed by a decision tree procedure to make predictions (Belgiu and Drăgu 2016; Breiman 2001). Our RF classifications were implemented in the R package ‘ranger’ (Wright and Ziegler 2017).

Training data for RF classifications were constructed by extracting shape, texture, and spectral features from the labelled segments within the orthomosaic (Table 2). The training data were used to construct three types of RF classifications to classify vegetation including (1) a pixel-based classification (referred to as ‘Pixel classification’), (2) an ‘OBIA’ classification and (3) a combination of OBIA and Pixel-based classifications (referred to as ‘combined classification’). We use ‘RF classifications’ throughout the manuscript as a hypernym for the Pixel-, OBIA- and Combined classifications.

For the Pixel-based classifications, pixel values of four spectral bands (i.e. green, red, red-edge and NIR of all pixels) within each segment were extracted. Neither textural nor shape features were used. For the object-based classifications, shape and texture features were calculated within each segment. This resulted in a total of 36 features (8 texture features x 4 bands + 4 shape features) for each segment. In the object-based classifications, average spectral characteristics were calculated for each segment. Lastly, the combined classifications were developed using the same 36 shape and textural features as for the OBIA classifications and the spectral information of the four bands of each pixel (following the Pixel classifications) within each segment. Therefore, in the combined classifications, all pixels within a segment had identical object features, but had different spectral characteristics.

**Table 2.** Parameters and features used to construct the object based (OBIA), Pixel based, and combined model. Training data for the models were generated from labelled segments of an ortho-image of a field trial.

Parameter	Feature	Description
Shape	Area	Area of each segment
	Compactness	Compactness of each segment
	Fractal dimension	Statistical index, that provides a ratio how segment boundaries change with scale (Mandelbrot 1982)
Texture	Length	Length of each segment
	Max	Maximum pixel value within each segment per band
	Mean of entropy	Mean entropy of pixels within each segment per band (Haralick, Dinstein, and Shanmugam 1973)
	Mean	Mean pixel value within each segment per band
	Mean SV <sup>a</sup>	Mean sum of variance of pixels within each segment per band (Haralick, Dinstein, and Shanmugam 1973)
	Min	Min pixel value of pixels within each segment per band
	SD <sup>b</sup> of entropy	Standard deviation of entropy within each segment per band (Haralick, Dinstein, and Shanmugam 1973)
	SD	Standard deviation of pixels value within each segment per band
Spectral features	SD of the sum of variance	Standard deviation of sum of variance within each segment per band (Haralick, Dinstein, and Shanmugam 1973)
	green, red, red-edge, NIR	All individual pixel values within each segment per band

The Pixel based model was constructed using spectral features of each pixel within segments, the OBIA model used spectral features, texture and shape features within segments and the combined model used spectral features of each pixel, spectral features, texture and shape features within segments.

<sup>a</sup>Abbreviation: SV, Sum of variance

<sup>b</sup>Abbreviation: SD, Standard deviation.

## 2.6. Random forest model classification training and validation

For each of the three RF classification methods, we developed two further models (referred to as either '5-class model' or '3-class model'). The 5-class models were used to categorize the percentage of the area covered by *clover*, *daisy*, *grass*, *soil* and *yarrow*. For the 3-class models we used the sum of *clover*, *daisy*, and *yarrow* to create a simplified 'weed'-class.

To quantify the balanced predictive accuracy of each trained RF (i.e. the accuracy is calculated independently for each class as the fraction of cases correctly classified, and these individual accuracy values are then averaged across all classes), a repeated five-fold cross-validation scheme was used for a total of 15 evaluations for each type of classification. Five-fold cross validation requires that for each evaluation, the dataset is randomly split into five subsets (Hastie, Tibshirani, and Friedman 2009). Four of the data subsets (i.e. 80% of the data) are used to train the algorithm and the remaining subset (20% of the data) is used to test predictions by the RF classifications. In the case of the combined classifications, all pixels that belonged to the same segment were sampled as indivisible units to avoid having pixels from the same segment in training and testing datasets (which would violate the principle of independence of the testing dataset, since all pixels within a segment share the same segment information). In all cases, the random sampling was stratified across classes to ensure the same relative proportions of classes as in the total dataset (i.e. the proportions of each class were maintained in each sample as in the total dataset) (Hastie, Tibshirani, and Friedman 2009). As the number of annotations per class differed (Table 1), each class was weighted during training by the inverse of the total number of annotations in that class, to avoid the negative effects of class imbalance. Confusion matrices were constructed to show the producer-, user-, OA of the RF classification predictions (Stehman 1997). Additionally, average accuracy (AA) and the kappa coefficient (K) were calculated.

## 2.7. Comparison of field- and random forest model classifications

Plot statistics were obtained by first using the trained RF classifications to categorize each segment of the whole orthomosaic. We then drew a polygon around each experimental plot, labelled the plot number and extracted data for each plot. Total weed cover and bare soil quantified by observed field measurements (i.e. point quadrat method for *weed*, *clover*, *daisy* and *yarrow* estimations and lightbox/ Turf Analyser method for *soil* estimation), were compared with values obtained using the predictions from all RF classifications (i.e. OBIA, Pixel and combined classifications for each 3-class model and 5-class model).

In order to evaluate the accuracy of the predictions for weed cover and bare soil we numerically evaluated the agreement between the observed and predicted values. Every scatterplot between the observed and predicted values suggested an exponential relationship. Thus, a logarithmic transformation was used to linearize the trend; as a result, a simple linear regression model was utilized to evaluate the log-transformed variables agreement. The AIC (Akaike Information Criterion) and MAE (Mean Absolute Error) were

computed as metrics to summarize model fit and used to determine the best model to explain agreement between observed and predicted data (Akaike 1974; Willmott and Matsuura 2005).

### 3. Results

#### 3.1. Data extraction per experimental unit

For each of the 136 experimental plots, we computed vegetation cover plot statistics based on the RF predictions following the example shown in Figure 2. The plot shown in Figure 2 was sown with Chewings fescue ('Musica') and clover. We calculated the surface area covered by each vegetation class.

#### 3.2. Pixel classification accuracy

The Pixel classification using the 3-class model resulted in the lowest accuracies of any of the 3-class model RF classifications, but was still able to correctly categorize grass, soil and weed cover with 90% to 95% OA (Table 3). The worst performing model (K = 83 and AA = 81%), based on 15 validation iterations, highlighted the difficulty in correctly classifying the weed class due to frequent confusion with grass (i.e. 19.7%, Table 4). We

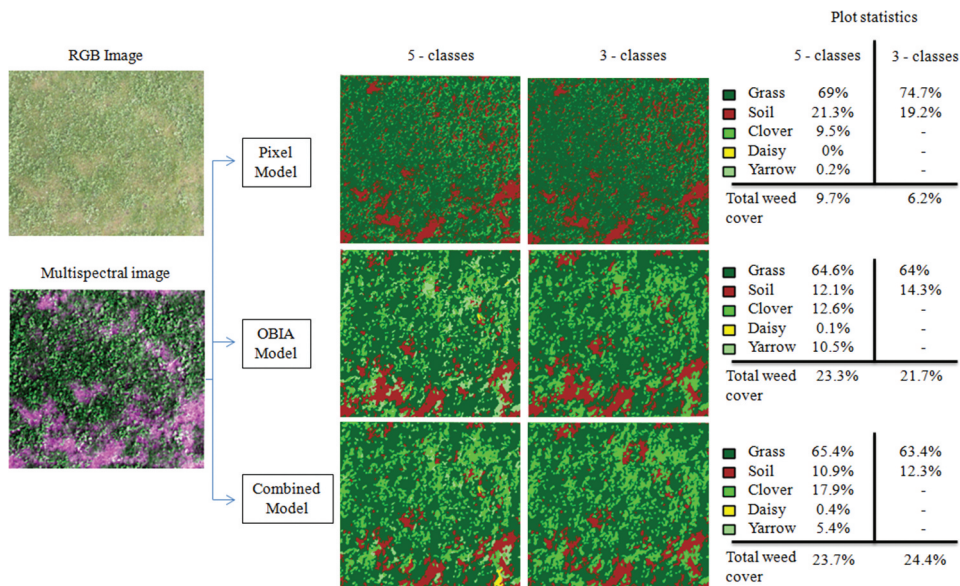


**Figure 2.** Visualization of an object-based- (OBIA), pixel-based and combined model approach to classify vegetation cover of field plots consisting of fescue cultivars and broadleaf turfgrass weeds. Figures show classification differences between either grass, soil, and weed (3-class model) or between clover, daisy, yarrow, grass, and soil (5-class model) and multispectral aerial images from the vegetation cover. Images were derived from one experimental plot established with Chewings fescue ('Musica') and clover.

**Table 3.** Accuracy assessment of object-based models (OBIA), Pixel and combined models to separate the percentage of area covered by different vegetation classes of a field trial. Results are grouped by two subset models with 3-class model (grass, soil, and weed) and 5-class model (clover, daisy, grass, soil, and yarrow) for each model.

		Percentages (%)		
		OBIA	Pixel	combined
3-class model	Grass	98 ( $\pm$ 2)	93 ( $\pm$ 0)	98 ( $\pm$ 3)
	Soil	99 ( $\pm$ 1)	95 ( $\pm$ 0)	98 ( $\pm$ 3)
	Weed	99 ( $\pm$ 1)	90 ( $\pm$ 1)	98 ( $\pm$ 3)
	Clover	82 ( $\pm$ 2)	77 ( $\pm$ 1)	92 ( $\pm$ 2)
5-class model	Daisy	88 ( $\pm$ 3)	77 ( $\pm$ 1)	98 ( $\pm$ 2)
	Grass	99 ( $\pm$ 1)	93 ( $\pm$ 0)	97 ( $\pm$ 3)
	Soil	100 ( $\pm$ 1)	96 ( $\pm$ 0)	86 ( $\pm$ 6)
	Yarrow	77 ( $\pm$ 5)	60 ( $\pm$ 1)	78 ( $\pm$ 6)

Accuracy is shown as averages (of 15 evaluations) and standard deviation is indicated as ' $\pm$ '.

**Table 4.** Confusion matrix of a 3-class model (grass, soil, and weed) object-based image analysis (OBIA) models, Pixel based models (Pixel) and a combination of both models (combined). Training data for the model was obtained from a segmented orthoimage of a field trial to investigate the competitiveness of fescue cultivars with broadleaf turfgrass weeds.

		Grass	Soil	Weed	Sum	User accuracy
OBIA	Grass	33	0	0	33	100%
	Soil	0	45	0	45	100%
	Weed	1	0	125	126	99.2%
	Sum	34	45	125	204	
	Producer accuracy	97.1%	100%	100%		
	Overall accuracy					99.4%
	Average accuracy					45.4%
Kappa x 100						99
Pixel	Grass	98331	1270	914	100515	97.8%
	Soil	696	7248	6	7950	91.2%
	Weed	628	9	2544	3181	80%
	Sum	99655	8527	3464	111646	
	Producer accuracy	98.7%	85%	73.4%		
	Overall accuracy					87.7%
	Average accuracy					81.0%
Kappa x 100						83
Combined	Grass	56865	0	24	56889	100%
	Soil	1408	11332	0	12740	88.9%
	Weed	0	0	3265	3265	100%
	Sum	58273	11332	3289	72894	
	Producer accuracy	97.6%	100%	99.3%	97.6%	
	Overall accuracy					97.6%
	Average accuracy					65.3%
Kappa x 100						94

present outcomes of the worst performing model in a confusion matrix to highlight where misclassification occurred; this information would not be evident by simply presenting average classification accuracies of all validation iterations.

The *5-class model* highlighted that *yarrow* was particularly difficult to detect, with a low accuracy of 60% (Table 3). The confusion matrix with the worst performing model of the Pixel classification ( $K = 77$  and  $AA = 80.5\%$ ) using the *5-class model* highlighted that the misclassification of plants belonging in the *weed* class was primarily attributed to the difficulties in classifying *yarrow*. *Yarrow* was more frequently misclassified as

*clover* or *grass* than it was correctly categorized, resulting in low producer and user accuracies of 19.2% and 18.4%, respectively. Additionally, *daisy* was misclassified as *clover* 27.5% of the time and *clover* was misclassified as *grass* 19.4% of the time (Table S1).

### 3.3. OBIA classification accuracy

The accuracy assessment of the OBIA classification using the 3-class model after 15 evaluation runs resulted in an average accuracy of 98% for *grass*, 99% for *soil*, and 99% for *weed* (Table 3). The confusion matrix with the lowest OA ( $K = 99$  and  $AA = 45.5\%$ ) of the 15 evaluations, showed that *weed* was confused with *grass* on one occasion, resulting in an OA of 99.4% (Table 4).

Further separating the *weed* class into species (*clover*, *daisy*, and *yarrow*) by the 5-class model decreased the OA of detecting weeds to 82.3% ( $\pm 3.3$ ) (Table 3), due to the difficulty in distinguishing among weeds. The confusion matrix of the evaluation with the lowest OA ( $K = 84$  and  $AA = 21.5\%$ ) showed that *yarrow* was the most difficult weed to classify. *Yarrow* was frequently (33.3%) misclassified as *clover* (Table S1). Nevertheless, using the 5-class model resulted in similar accuracy of classification of the *soil* and *grass* classes.

### 3.4. Combined classification accuracy

The combined classification with the 3-class model achieved an OA of 98% (Table 3). *Weed* and *grass* were detected with 100% user accuracy, while *grass* was confused with *soil* 11.6% of the time in the worst performing confusion matrix ( $K = 94$  and  $AA = 65.3\%$ ) (Table 4).

Separating the *weed* class into *clover*, *daisy* and *yarrow* resulted in a drop of accuracy, with *yarrow* contributing most to any misclassification. Overall classification accuracy for *yarrow* was 78%, and *daisy* was correctly classified with 98% accuracy (Table 3). In the worst performing confusion matrix, *yarrow* was mainly misclassified as *clover* by 32.2% of the time. Furthermore, *daisy* was frequently misclassified as *yarrow* 35.6% of the time (Table S1).

### 3.5. Feature importance of random forest model classifications

Pixel values for each vegetation type indicated that *soil* in particular showed lower values in the NIR and red-edge spectra (Figure S2). Within all bands, *clover* had similar pixel values as *daisy*, with overall differences most prominent in the red band. *Grass* showed unique pixel values in the NIR and red-edge band, being lower than any of the *weeds* and higher than *soil*. In the red band, *grass* showed the lowest mean pixel values of all classes. Pixel values of *yarrow* were similar to those of *daisy* and *clover* in particular in all bands.

For the Pixel classification using the 3-class model, the green band was most important to detect features closely followed by the red band with 17% less relative importance (data not shown). Red edge and NIR were the least important features with 72.9% and 77% less relative importance compared to the green band. For the 5-class model, Pixel

classification differences were more prominent with the red band being most important closely followed by the green band (2% less relative importance) and 86% for red edge and NIR (data not shown).

For both the *3-class* and *5-class models* OBIA classifications, mean green pixel values for each segment contributed most to the classification of vegetation type (Figure 3). In general, the mean pixel values of each band were among the seven most important features for both models. Furthermore, the sum of variance (SV) of pixels values proved to be an important feature, particularly in the green band of the *5-class model*. Also, the maximum NIR feature was an important feature to classify vegetation in both modes. The OBIA-specific shape parameters scored low in importance, and for the *5-class model*, all of the shape parameters were the least important features.

For the *3-class model* combined classification, shape parameters such as fractal dimension and length proved to be the most important features (Figure 4). This was followed by the mean pixel values for green, SV for green and red edge. Eight features were of no relative importance for classifying vegetation. For the *5-class model* combined classification, there was less of a difference in importance among the features, with only one feature (the green band) not contributing to the classification of vegetation.

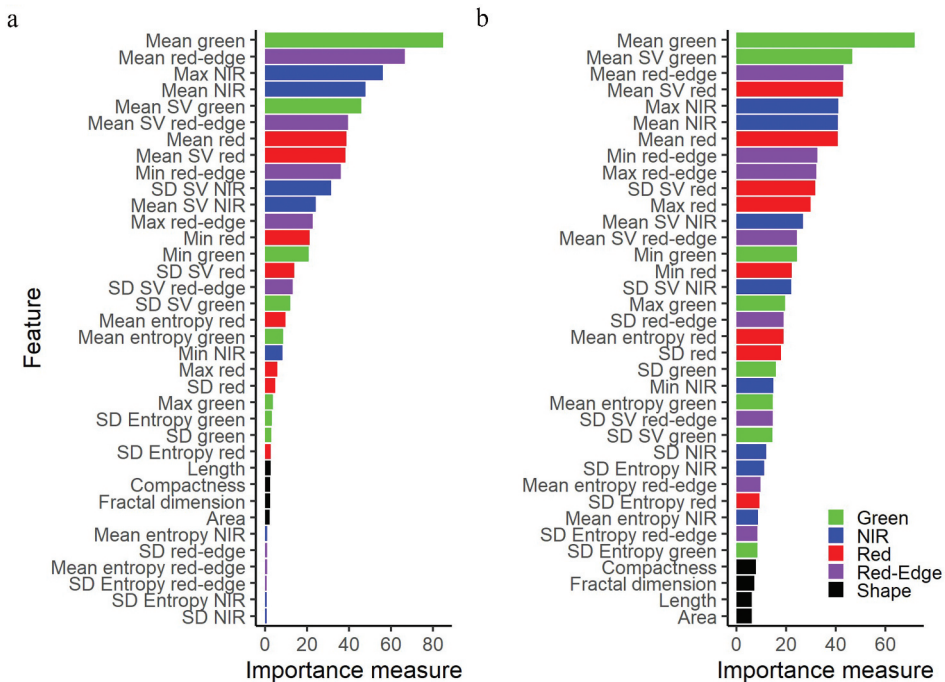


**Figure 3.** Feature importance charts of (A) a 3-class model (grass, soil, and weed) object-based image analysis (OBIA) model and (B) 5-class model (clover, daisy, grass, soil, and yarrow) OBIA model to quantify vegetation cover in a fescue cultivars and broadleaf weed field trial. Importance measure is a dimensionless/ relative measurement. Colours indicate the spectral bands green, blue (NIR), red, and object-based shape parameters. NIR, near infrared; SV, Sum of variance; SD, Standard deviation.

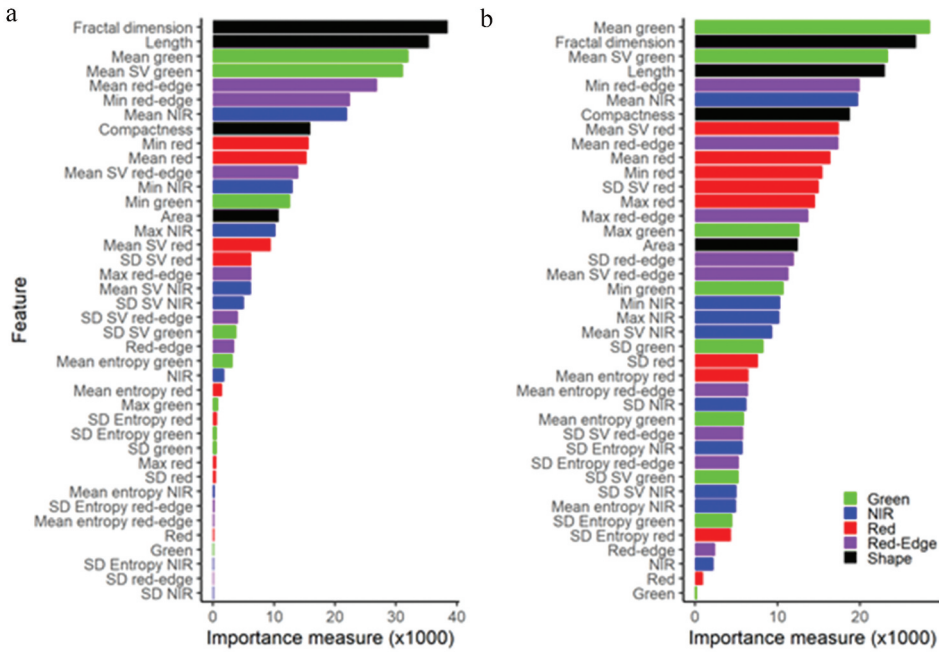


**Figure 4.** Feature importance charts of (A) a 3-class model (grass, soil, and weed) combined- image analysis model (OBIA shape parameters and spectral features of Pixles) and (B) 5-class model (clover, daisy, grass, soil, and yarrow) combined- image analysis model to quantify vegetation cover in a fescue cultivars and broadleaf weed field trial. Importance measure is a unit less/ relative measurement. Colours indicate the spectral bands green, blue (NIR), red, and object- based shape parameters. NIR, near infrared; SV, Sum of variance; SD, Standard deviation.

**3.6. Comparison of observed and predicted data**

The least agreement between observed and predicted data (high AIC and MAE) used to estimate weed cover were reported in plots sown with grass only (Grass controls) for all RF classifications (Table 5). In plots sown with weed treatments, both OBIA and the combined classifications showed better agreement with observed data compared to the Pixel classifications for both 3-class and 5-class models. Differences between OBIA and combined classifications were marginal except for the 3-class models' detection of weed cover in mixtures. In mixtures, OBIA classification using the 3-class model performed worse (AIC = 49.4) than the 5-class model (AIC = 28.10). The MAE for OBIA and the combined classifications also showed that both classification methods performed equally in detecting weed cover, with no clear difference between 3-class and 5-class models.

For soil estimations, we generally observed better agreement between methods, with overall lower AIC and MAE compared to estimations of weed cover for all models. However, the Pixel classifications again performed worse than the OBIA and combined classifications, except in plots sown with yarrow, where there was similar agreement between all RF classifications and observed data (AIC between 31.1 and 33.1). The MAE between predicted and observed data in plots sown with yarrow were the same (0.26–0.27). Overall, combined classification using the 5-class model scored the lowest AIC scores

**Table 5.** Comparison of remotely sensed total weed cover estimates with field observations using Akaike information criterion (AIC) and Mean absolute error (MAE) on log-transformed values. Methods to estimate weed cover included ground measurements with a 100-point quadrat and analysis of aerial multispectral images using object-based image analysis (OBIA) models, Pixel based models (Pixel) and a combination of both models (combined), for 3-class model (grass, soil, and weed) and 5-class model (clover, daisy, grass, soil, and yarrow).

	Sowed treatment	3-class model			5-class model		
		Pixel	OBIA	Combined	Pixel	OBIA	Combined
AIC*	Clover	42.7	27.5	26.2	42.4	27.5	26.6
	Daisy	48.6	34.1	34.7	47.5	34.6	34.1
	Yarrow	42.8	37.6	37.1	42.1	37.4	37.4
	Mixture	54.5	26.4	28.8	52.9	28.1	29.9
	Grass c.*	52.2	49.4	50.1	52.1	50.2	50.0
MAE*	Clover	0.37	0.27	0.26	0.36	0.27	0.26
	Daisy	0.39	0.29	0.29	0.38	0.29	0.29
	Yarrow	0.32	0.29	0.29	0.32	0.29	0.29
	Mixture	0.43	0.25	0.26	0.42	0.26	0.27
	Grass c.*	0.53	0.47	0.49	0.52	0.48	0.49

\*MAE = Mean Absolute Error; AIC = Akaike Information Criterion; Grass c. = Grass control.

(162.2), closely followed by combined classification using the *3-class model* and OBIA classification using the *5-class model* (164.1 and 164.2 respectively). The MAE for combined and OBIA classification using the *3-class* and *5-class models* were similar.

#### 4. Discussion

Using our RF classifications, we were able to successfully distinguish green vegetation cover (grass and weeds) from non-vegetation cover (bare soil). The OBIA classification using the *5-class model* was able to classify soil with 100% accuracy due to the high reflectance of green vegetation in the NIR portion of the electromagnetic spectrum in comparison to the lower reflectance of soil. Digital analysis of the green fraction of pixels has been used by other researchers to measure cover and quality of turfgrasses (Karcher and Richardson 2013). However, the methodology used in their study was not able to distinguish between weeds and grasses because both classes have similar reflectance values in the green portion of the electromagnetic spectrum. Identifying plant species from within a landscape of green vegetation is generally more complex and challenging (Lamb and Brown 2001). We encountered these challenges with regard to *clover*, which had similar pixel values at all measured bands (Figure S2). As reported by Casapia et al. (2020), we found that the mean green pixel values within segments were an important feature for OBIA classifications (Figure 3). The average spectral reflectance within segments was used, whereas the shape parameters of the objects did not appear to be important features. The OBIA classifications performed much better than the Pixel model, indicating that even less important shape parameters led to better classification accuracy (Tables 4 & Tables 6). For the combined classification, all individual pixels within segments were classified. In that case, we observed that the shape parameters such as fractal dimension and length were the most important features, particularly for the *3-class model*. However, the shift in relative importance of shape parameters in OBIA classifications compared to the combined classifications, did

**Table 6.** Akaike information criterion (AIC) and Mean absolute error (MAE) for log transformed values of two methods for estimating bare soil in between vegetation cover using aerial image analysis of a field trial. Ground measurements included, single picture analysis of 136 plots captured with a RGB camera and subsequent analysis with Turf Analyser software. Aerial multispectral images were analysed using object-based models, Pixel-based models (Pixel) and a combined model (combined) for a 3-class model (grass, soil, and weed) and a 5-class model (clover, daisy, grass, soil, and yarrow). Data was log transformed.

	Sowed treatment	3-class model			5-class model		
		Pixel	OBIA	Combined	Pixel	OBIA	Combined
AIC*	Clover	45.6	35.7	32.3	45.2	34.5	31.7
	Daisy	62.5	47.6	45.8	62.6	42.6	44.1
	Yarrow	33.1	33.0	31.9	32.4	32.8	31.1
	Mixture	43.0	29.4	32.1	41.7	29.5	32.6
	Grass c.*	31.9	26.3	22.0	30.1	24.8	22.7
MAE*	Clover	0.33	0.30	0.26	0.33	0.29	0.26
	Daisy	0.49	0.40	0.38	0.49	0.36	0.36
	Yarrow	0.26	0.26	0.27	0.26	0.26	0.27
	Mixture	0.35	0.27	0.28	0.34	0.26	0.28
	Grass c.*	0.31	0.26	0.23	0.30	0.25	0.23

\*MAE = Mean Absolute Error; AIC = Akaike Information Criterion; Grass c. = Grass control.

not significantly alter the predictive accuracy of the models. Both models showed high accuracy when using the *3-class model* (98–99%), and while the OBIA *5-class model* was superior at detecting *grass* and *soil*, the combined model scored higher accuracies for detecting *clover* and *daisy* (10% more accurate for both classes). Hence, if the overall goal is to detect general weed cover, the object-based classification approach is recommended.

When comparing cover estimations based on industry-standard in-field measurements (observed) and the RF classifications (predicted), we found that agreement between observed and predicted estimates of weed cover was particularly good in plots sown with daisy and mixtures for both OBIA and combined classifications (Table 5). This could be due to the fact that daisy growth flat on the surface with sharp leaf edges. Compared to the other tested weed species daisy clearly stood out. A weed species that can be easily separated visually is also easier to detect in an image analysis approach. The highest discrepancy between observed and predicted estimates for both OBIA and the combined classifications occurred in plots sown without weeds (grass controls). For estimates of *soil* cover we found the opposite to be true, with the best agreement between observed and predicted values found in plots sown with grass only and the highest discrepancy found in plots sown with daisy, for OBIA and combined classifications. Some of the weed species such as yarrow do not have a solid leaf blade but a feather type of blade. Because of the segmentation process an object like a yarrow leaf could potentially be classified as soil if the reflectance of the soil through the yarrow leaf blade overrides the reflectance of the yarrow leaf blade itself. Grasses such as fescues have an upright growth habit and because the camera was pointed vertically at the plot, it is likely that in grass control plots the clear edges between soil and grass patches were visible, leading to high classification accuracy of soil in grass control plots.

Using remote sensing to detect weeds in regularly mowed turfgrass is generally challenging because of the small size of individual weed plants, which requires high resolution imagery. In our study, we found *yarrow* to be a particularly problematic weed to detect, which was most likely due to its similarity in leaf shape and spectral features to grasses (Fig. S2). Compared to natural grasslands, where vegetation cover and characteristics show strong seasonality (Zillmann et al. 2014), cover of turfgrass is much less dynamic due to the intense management regimes. This consistent and uniform cover is better suited to classification models such as those developed in this study and result in improved classification accuracy. Due to the mowing regime of turfgrass, we expect spectral and shape characteristics to be more seasonally uniform and suggest that our results could be applicable throughout the entire season. More research is needed to confirm this suggestion.

In this study we focused on three weed species that commonly occur on golf courses, however there are many more. Future research efforts should focus on examining the influence of different weed species on the predictive accuracy of image analysis approaches. For the purposes of identifying weed cover, our results are highly encouraging, given the high accuracy (98–99%) of the object-based classification that grouped all weeds into a single class (*3-class model*). Apparently, the three contrasting weed species used in this study share common characteristics that can be successfully captured by our method and are considerably different from grass characteristics. The spectral reflectance of all features used to construct the models (Fig. S2) suggests that main differences between weeds and grass are in mean red entropy, shape parameters and mean green. Accordingly, we anticipate that our method may also be successful in identifying weed species that have a growth form similar to clover, daisy, and to a lesser degree, yarrow. To what extent our results can be generalized to other weed species is an open question that is of interest for future research.

In conclusion, our research demonstrated that object-based classification is a useful tool for weed detection, especially when compared to the currently employed time consuming in-field measurement with a point quadrat and lightbox. Our study showed that using texture features (OBIA- and combined model), the *3-class models* classified soil, weed, and grass with 98–99% accuracy, and the *5-class models* discriminated between soil, grass, and the three weed cover types with 81–80% accuracy. Agreement between predicted estimates of vegetation type and bare soil and observed estimates obtained using point quadrat and Turf analyser methods varied depending on the grass/weed seeding treatment.

## Acknowledgements

First and second author have contributed equally to this report. We especially thank Dr. Rossana Sallenave for her help with the manuscript. Financial support of this project was provided by the Turfgrass University Research Foundation (TuRF), Nederlandse Golf Federatie (NGF), Nederlandse Vereniging van Golfaccommodaties (NVG), and Nederlandse Greenkeepers Associatie (NGA). We are also grateful for the contribution of Barenbrug Holland B.V. in Nijmegen, Netherlands.

## Disclosure statement

No potential conflict of interest was reported by the author(s).

## Funding

This work was supported by the Turfgrass University Research Foundation, The Netherlands. [n/a].

## ORCID

Bernd Leinauer  <http://orcid.org/0000-0002-3700-2005>

## References

- Akaike, H. 1974. "A New Look at the Statistical Model Identification." *IEEE Transactions on Automatic Control* 19 (6): 716–723. doi:10.1109/TAC.1974.1100705.
- Aktar, W., D. Sengupta, and A. Chowdhury. 2009. "Impact of Pesticides Use in Agriculture: Their Benefits and Hazards." *Interdisciplinary Toxicology* 2 (1): 1–12. doi:10.2478/v10102-009-0001-7.
- Alberg, A. J., J. W. Park, B. W. Hager, M. V. Brock, and M. Diener-West. 2004. "The Use of 'Overall Accuracy' to Evaluate the Validity of Screening or Diagnostic Tests." *Journal of General Internal Medicine* 19 (5): 460–465. doi:10.1111/j.1525-1497.2004.30091.x.
- Analyzer, T. 2018. "Analyze Plant Health." <http://turfanalyzer.com>
- Belgiu, M., and L. Drăgu. 2016. "Random Forest in Remote Sensing: A Review of Applications and Future Directions." *ISPRS Journal of Photogrammetry and Remote Sensing* 114: 24–31. doi:10.1016/j.isprsjprs.2016.01.011.
- Blaschke, T., G. J. Hay, M. Kelly, S. Lang, P. Hofmann, E. Addink, R. Queiroz Feitosa, et al. 2014. "Geographic Object-Based Image Analysis - Towards a New Paradigm." *ISPRS Journal of Photogrammetry and Remote Sensing* 87 :180–191. doi:10.1016/j.isprsjprs.2013.09.014.
- Breiman, L. 2001. "Random Forests." *Machine Learning* 45 (1): 5–32. doi:10.1023/A:1010933404324.
- Brodley, C. E., and M. A. Friedl. 1997. "Decision Tree Classification of Land Cover from Remotely Sensed Data." *Remote Sensing of Environment* 61 (3): 399–409. doi:10.1016/S0034-4257(97)00049-7.
- Brown, L. G. 1992. "A Survey of Image Registration Techniques." *ACM Computing Surveys* 24 (4): 325–376. doi:10.1145/146370.146374.
- Bunderson, L. D., P. G. Johnson, K. L. Kopp, and A. Van Dyke. 2009. "Tools for Evaluating Native Grasses as Low Maintenance Turf." *HortTechnology* 19 (3): 626–632. doi:10.21273/hortsci.19.3.626.
- Busey, P. 2003. "Cultural Management of Weeds in Turfgrass: A Review." *Crop Science* 43 (6): 1899–1911. doi:10.2135/cropsci2003.1899.
- Casapia, X. T., L. Falen, H. Bartholomeus, R. Cárdenas, G. Flores, M. Herold, E. N. H. Coronado, and T. R. Baker. 2020. "Identifying and Quantifying the Abundance of Economically Important Palms in Tropical Moist Forest Using UAV Imagery." *Remote Sensing* 12 (1): 1–26. doi:10.3390/RS12010009.
- Dahl Jensen, A. M., O. Bühler, A. Kvalbein, and T. S. Aamlid. 2017. "Evaluation of the Occurrence of Turfgrasses and Weeds after Repeated Overseeding on Fairways." *International Turfgrass Society Research Journal* 13 (1): 389–393. doi:10.2134/itsrj2016.10.0837.
- De Prado, R. A., and A. R. Franco. 2004. "Cross-Resistance and Herbicide Metabolism in Grass Weeds in Europe: Biochemical and Physiological Aspects." *Weed Science* 52 (3): 441–447. doi:10.1614/p2002-168a.
- European Parliament. 2009. "Directive 2009/128/EC of the European Parliament and the Council of 21 October 2009 Establishing a Framework for Community Action to Achieve the Sustainable Use of Pesticides." *October*. doi:10.3000/17252555.L\_2009.309.
- Gašparović, M., M. Zrinjski, Đ. Barković, and D. Radočaj. 2020. "An Automatic Method for Weed Mapping in Oat Fields Based on UAV Imagery." *Computers and Electronics in Agriculture* 173: 105385. doi:10.1016/j.compag.2020.105385.

- Gaussoin, R. E., and B. E. Branham. 1989. "Influence of Cultural Factors on Species Dominance in a Mixed Stand of Annual Bluegrass/Creeping Bentgrass." *Crop Science* 29 (2): 480–484. doi:10.2135/cropsci1989.0011183X002900020048x.
- Gómez, C., J. C. White, and M. A. Wulder. 2016. "Optical Remotely Sensed Time Series Data for Land Cover Classification: A Review." *ISPRS Journal of Photogrammetry and Remote Sensing* 116: 55–72. doi:10.1016/j.isprsjprs.2016.03.008.
- GRASS Development Team. 2017. "Geographic Resources Analysis Support System (GRASS)." Open Source Geospatial Foundation. <http://grass.osgeo.org>
- Haralick, R. M., I. Dinstein, and K. Shanmugam. 1973. "Textural Features for Image Classification." *IEEE Transactions on Systems, Man and Cybernetics* 3 (6): 610–621. doi:10.1109/TSMC.1973.4309314.
- Hastie, T., R. Tibshirani, and J. Friedman. 2009. *The Elements of Statistical Learning: Data Mining, Inference, and Prediction*. Springer Science & Business Media. doi:10.1007/978-0-387-84858-7.
- Heap, I. 2014. "Global Perspective of Herbicide-Resistant Weeds." *Pest Management Science* 70 (9): 1306–1315. doi:10.1002/ps.3696.
- Horst, G. L., M. C. Engelke, and W. Meyers. 1984. "Assessment of Visual Evaluation Techniques 1." *Agronomy Journal* 76 (4): 619–622. doi:10.2134/agronj1984.00021962007600040027x.
- Hsieh, P. F., L. C. Lee, and N. Y. Chen. 2001. "Effect of Spatial Resolution on Classification Errors of Pure and Mixed Pixels in Remote Sensing." *IEEE Transactions on Geoscience and Remote Sensing* 39 (12): 2657–2663. doi:10.1109/36.975000.
- Hutto, K. C., D. R. Shaw, J. D. Byrd, and R. L. King. 2006. "Differentiation of Turfgrass and Common Weed Species Using Hyperspectral Radiometry." *Weed Science* 54 (2): 335–339. doi:10.1614/ws-05-116r.1.
- Jiménez-Brenes, F. M., F. López-Granados, J. Torres-Sánchez, J. M. Peña, P. Ramírez, I. L. Castillejo-González, and A. I. De Castro. 2019. "Automatic UAV-Based Detection of *Cynodon Dactylon* for Site-Specific Vineyard Management." *PLoS ONE* 14 (6): 6. doi:10.1371/journal.pone.0218132.
- Karcher, D. E., and M. D. Richardson. 2013. "Digital Image Analysis in Turfgrass Research." *Turfgrass: Biology, Use and Management* 56: 1133–1149.
- Kaur, N., J. L. Gillett-Kaufman, S. A. Gezan, and E. A. Buss. 2016. "Association between *Blissus insularis* Densities and St. Augustinegrass Lawn Parameters in Florida." *Crop, Forage & Turfgrass Management* 2 (1): 1–5. doi:10.2134/cftm2016.0015.
- Kim, K. H., E. Kabir, and S. A. Jahan. 2017. "Exposure to Pesticides and the Associated Human Health Effects." *Science of the Total Environment* 575: 525–535. doi:10.1016/j.scitotenv.2016.09.009.
- Laganieri, R. 2000. "Compositing a Bird's Eye View Mosaic." *Proc. Conf. Vision Interface* 1: 382–387.
- Lamb, D. W., and R. B. Brown. 2001. "PA—Precision Agriculture: Remote-Sensing and Mapping of Weeds in Crops." *Journal of Agricultural Engineering Research* 78 (2): 117–125. doi:10.1006/jaer.2000.0630.
- Larsen, S. U., P. Kristoffersen, and J. Fischer. 2004. "Turfgrass Management and Weed Control without Pesticides on Football Pitches in Denmark." *Pest Management Science* 60 (6): 579–587. doi:10.1002/ps.845.
- Latimer, J. G., S. K. Braman, R. B. Beverly, P. A. Thomas, J. T. Walker, B. Sparks, R. D. Oetting, et al. 1996. "Reducing the Pollution Potential of Pesticides and Fertilizers in the Environmental Horticulture Industry: II. Lawn Care and Landscape Management." *HortTechnology* 6 (2): 222–232. doi:10.21273/HORTTECH.6.2.115.
- Laycock, R. W. 1980. "A New Optical Point Quadrant Frame for the Estimation of Cover in Close Mown Turf." *Journal of the Sports Turf Research Institute* 56: 91–92.
- Leinauer, B., D. M. VanLeeuwen, M. Serena, M. Schiavon, and E. Sevostianova. 2014. "Digital Image Analysis and Spectral Reflectance to Determine Turfgrass Quality." *Agronomy Journal* 106 (5): 1787–1794. doi:10.2134/agronj14.0088.
- Ma, Y., H. Wu, L. Wang, B. Huang, R. Ranjan, A. Zomaya, and W. Jie. 2015. "Remote Sensing Big Data Computing: Challenges and Opportunities." *Future Generation Computer Systems* 51: 47–60. doi:10.1016/j.future.2014.10.029.
- Mandelbrot, B. 1982. *The Fractal Geometry of Nature*. New York: W.H. Freeman.
- Marth, P. C., and J. W. Mitchell. 1944. "2,4-Dichlorophenoxyacetic Acid as a Differential Herbicide." *Botanical Gazette* 106 (2): 224–232. doi:10.1086/335289.

- McCarthy, L. B., and T. R. Murphy. 1994. *Control of Turfgrass Weeds*. Madison, WI: ASA, CSSA, and SSSA Books.
- McElroy, S. J., and D. Martins. 2013. "Use of Herbicides on Turfgrass." *Planta Daninha* 31 (2): 455–467. doi:10.1590/S0100-83582013000200024.
- Mulla, D. J. 2013. "Twenty Five Years of Remote Sensing in Precision Agriculture: Key Advances and Remaining Knowledge Gaps." *Biosystems Engineering* 114 (4): 358–371. doi:10.1016/j.biosystemseng.2012.08.009.
- National Turfgrass Evaluation Program. 2020. "The National Turfgrass Evaluation Program: Assessing New and Improved Varieties." <https://www.ntep.org/contents2.shtml>
- Nijp, J., A. J. A. M. Temme, G. A. K. van Voorn, L. Kooistra, G. M. Hengeveld, M. B. Soons, A. J. Teuling, and J. Wallinga. 2019. "Spatial Early Warning Signals for Impending Regime Shifts: A Practical Framework for Application in Real-World Landscapes." *Global Change Biology* 25 (6): 1905–1921. Blackwell Publishing Ltd. doi:10.1111/gcb.14591.
- Nitze, I., U. Schulthess, and H. Asche. 2012. "Comparison of Machine Learning Algorithms Random Forest, Artificial Neuronal Network and Support Vector Machine to Maximum Likelihood for Supervised Crop Type Classification." In *Proceedings of the 4th Conference on GEographic Object-Based Image Analysis – GEOBIA 2012*, Rio de Janeiro, Brazil. 35–40. <https://www.researchgate.net/publication/275641579>
- Olmstead, M. A., R. Wample, S. Greene, and J. Tarara. 2004. "Nondestructive Measurement of Vegetative Cover Using Digital Image Analysis." *HortScience* 39 (1): 55–59. doi:10.21273/hortsci.39.1.55.
- Proctor, C. A., D. V. Weisenberger, and Z. J. Reicher. 2015. "Kentucky Bluegrass and Perennial Ryegrass Mixtures for Establishing Midwest Lawns." *HortScience* 50 (1): 137–140. doi:10.21273/hortsci.50.1.137.
- Roosjen, P. P. J., B. Brede, J. M. Suomalainen, H. M. Bartholomeus, L. Kooistra, and J. G. P. W. Clevers. 2018. "Improved Estimation of Leaf Area Index and Leaf Chlorophyll Content of a Potato Crop Using Multi-Angle Spectral Data – Potential of Unmanned Aerial Vehicle Imagery." *International Journal of Applied Earth Observation and Geoinformation* 66: 14–26. doi:10.1016/j.jag.2017.10.012.
- Stehman, S. V. 1997. "Selecting and Interpreting Measures of Thematic Classification Accuracy." *Remote Sensing of Environment* 62 (1): 77–89. Elsevier. doi:10.1016/S0034-4257(97)00083-7.
- Tang, J. L., X. Q. Chen, R. H. Miao, and D. Wang. 2016. "Weed Detection Using Image Processing under Different Illumination for Site-Specific Areas Spraying." *Computers and Electronics in Agriculture* 122: 103–111. doi:10.1016/j.compag.2015.12.016.
- Thorp, K. R., and L. F. Tian. 2004. "A Review on Remote Sensing of Weeds in Agriculture." *Precision Agriculture* 5 (5): 477–508. doi:10.1007/s11119-004-5321-1.
- Trenholm, L. E., R. N. Carrow, and R. R. Duncan. 1999. "Relationship of Multispectral Radiometry Data to Qualitative Data in Turfgrass Research." *Crop Science* 39 (3): 763–769. Crop Science Society of America. doi:10.2135/cropsci1999.0011183X003900030025x.
- Voight, T. B., T. W. Fermanian, and J. E. Haley. 2001. "Influence of Mowing and Nitrogen Fertility on Tall Fescue Turf." *International Turfgrass Society Research Journal* 9 (2): 953–956.
- Weis, M., T. Rumpf, R. Gerhards, and L. Plümer. 2009. "Comparison of Different Classification Algorithms for Weed Detection from Images Based on Shape Parameters." *Bornimer Agrartechnische Berichte* 69: 53–64.
- Willmott, C. J., and K. Matsuura. 2005. "Advantages of the Mean Absolute Error (MAE) over the Root Mean Square Error (RMSE) in Assessing Average Model Performance." *Climate Research* 30 (1): 79–82. Inter-Research. doi:10.3354/cr030079.
- Wright, M. N., and A. Ziegler. 2017. "Ranger: A Fast Implementation of Random Forests for High Dimensional Data in C++ and R." *Journal of Statistical Software* 77 (1): 1–17. American Statistical Association. doi:10.18637/jss.v077.i01.
- Yang, G., J. Liu, C. Zhao, Z. Li, Y. Huang, H. Yu, B. Xu, et al. 2017. "Unmanned Aerial Vehicle Remote Sensing for Field-Based Crop Phenotyping: Current Status and Perspectives." *Frontiers in Plant Science* 8 (1111): 1–26. doi:10.3389/fpls.2017.01111.

- Yu, J., A. W. Schumann, S. M. Sharpe, L. Xuehan, and N. S. Boyd. 2020. "Detection of Grassy Weeds in Bermudagrass with Deep Convolutional Neural Networks." *Weed Science* 68 (5): 1–8. doi:[10.1017/wsc.2020.46](https://doi.org/10.1017/wsc.2020.46).
- Zhang, C., and J. M. Kovacs. 2012. "The Application of Small Unmanned Aerial Systems for Precision Agriculture: A Review." *Precision Agriculture* 13 (6): 693–712. doi:[10.1007/s11119-012-9274-5](https://doi.org/10.1007/s11119-012-9274-5).
- Zillmann, E., A. Gonzalez, E. J. Montero Herrero, J. Van Wavelaer, T. Esch, M. Keil, H. Weichelt, and A. M. Garzón. 2014. "Pan-European Grassland Mapping Using Seasonal Statistics from Multisensor Image Time Series." *IEEE Journal of Selected Topics in Applied Earth Observations and Remote Sensing* 7 (8): 3461–3472. Institute of Electrical and Electronics Engineers. doi:[10.1109/JSTARS.2014.2321432](https://doi.org/10.1109/JSTARS.2014.2321432).